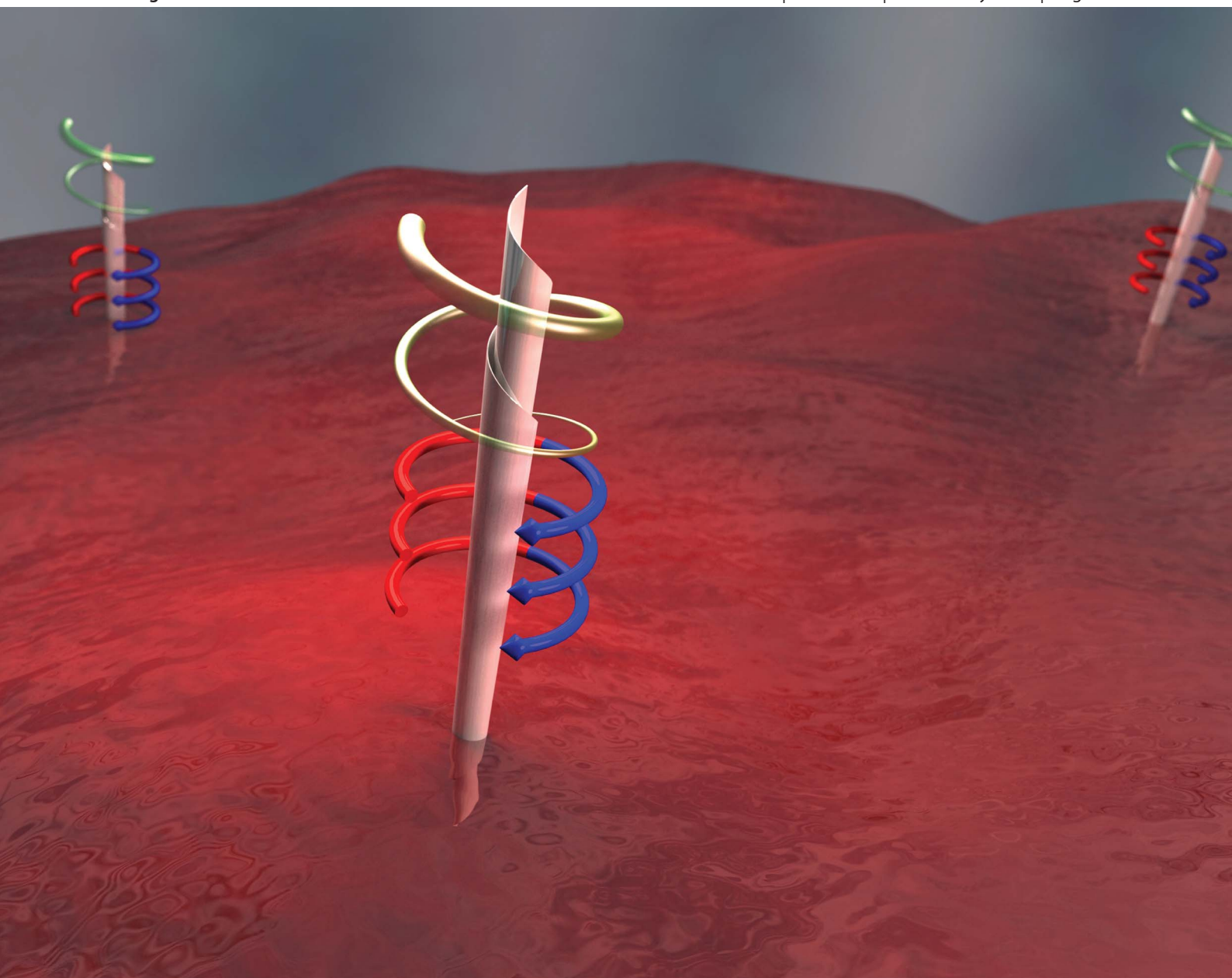


Nanoscale

www.rsc.org/nanoscale

Volume 5 | Number 4 | 21 February 2013 | Pages 1237–1696



Includes a collection of articles on the theme of self-propelled nano and microsystems

ISSN 2040-3364

RSC Publishing

COMMUNICATION

Sanchez *et al.*

Rolled-up magnetic microdrillers:
towards remotely controlled minimally
invasive surgery



NCNST



2040-3364 (2013) 5:4;1-K

Rolled-up magnetic microdrillers: towards remotely controlled minimally invasive surgery†

Cite this: *Nanoscale*, 2013, 5, 1294Received 18th September 2012
Accepted 15th October 2012

DOI: 10.1039/c2nr32798h

www.rsc.org/nanoscale

Wang Xi,‡^a Alexander A. Solovov,‡^{ab} Adithya N. Ananth,^a David H. Gracias,^c
Samuel Sanchez^{*a} and Oliver G. Schmidt^{ad}

Self-folded magnetic microtools with sharp ends are directed at enabling drilling and related incision operations of tissues, *ex vivo*, in a fluid with a viscosity similar to that of blood. These microtools change their rotation from a horizontal to a vertical one when they are immersed into a rotational magnetic field. Novel self-assembly paradigms with magnetic materials can enable the creation of remotely controlled and mass-produced tools for potential applications in minimally invasive surgery.

With advances in micro and nanotechnology, it has been argued that the creation and implementation of dynamic micro- and nanoscale mechanized structures could revolutionize minimally invasive surgery (MIS). The first step towards enabling this vision is to create small tools that can mimic the functionality of larger tools utilized in surgery.^{1–5} In addition, it is necessary to develop methods so that these tools can be guided and implemented in a tether-free manner. One class of tools in surgery are sharp surgical instruments such as scalpels or surgical drills that are widely utilized for making incisions. Some of these surgical instruments are enabled by electromagnetic motors on the macroscale, but it can be very challenging to harness the energy required to provide drilling or localized incisions at smaller size scales and in a tether-free manner.

One approach to power micro- and nanoscale tools involves the catalytic conversion of chemical energy (energy-rich molecules in solution) into mechanical energy.^{5–18} However, a significant limitation of these artificially designed micro- and nanomotors, engines

and nanotools is that they require toxic fuels (hydrogen peroxide, hydrazine, and strong acids) and thus they cannot be used *in vivo*.^{5,11–14} In the instances where less toxic fuels have been utilized, their applicability in surgically relevant procedures has yet to be demonstrated.^{16,18–20} For example, previously, our own group has reported sharp InGaAs/GaAs/Cr/Pt nanotools;⁵ however, a hydrogen peroxide fuel solution was required for self-propulsion, which cannot be implemented *in vivo* due to toxicity concerns. An attractive approach relies on the fabrication of “fuel-free” micro-nanotools driven by external fields, *e.g.* those powered by external magnetic fields.^{21–26} Recently, the enzymatically triggered and tetherless thermobiochemical actuation of miniaturized grippers and tools, magnetically guided into glass tubes and acrylic liver models, was demonstrated.^{2–4} Such miniaturized and remote-controlled microtools may have high potential for *in vivo* applications in the near future in the circulatory, the urinary and the central nervous systems.²⁵ However, to fabricate cost-effective and operative MIS devices, scientists need to make use of fabrication techniques that enable mass production of non-trivially shaped three-dimensional structures, often with multiple classes of materials. In this context, rolled-up nanotechnology²⁷ – previously envisioned for nanodriller applications⁵ – meets the aforementioned requirements.

In this work, we demonstrate that tubular Ti/Cr/Fe microdrillers containing sharp tips can be applied for mechanical drilling operations of porcine liver tissue *ex vivo*. An external rotational magnetic field is used to remotely locate and activate the microdrillers in a solution with a viscosity comparable to that of biological fluids (*e.g.*, blood). Changes in the frequency of the rotating magnetic field result in the switching of the rotational orientation of the microdriller from a horizontal to a vertical one, which lifts the tubes and makes them applicable for drilling. Hence, we show that magnetic rolled-up microtubes can be used for directed drilling of holes in soft matter, using porcine liver tissue as a model system.

Fig. 1A shows a schematic of the sandwiched structure of the nanomembranes on a sacrificial polymer (photoresist) patterned on a silicon substrate. The trapezia shaped patterns were prepared using standard photolithography and followed by angular e-beam deposition of Ti/Cr/Fe (5/5/5 nm) layers, similar to those previously

^aInstitute for Integrative Nanosciences, IFW Dresden, Helmholtzstr 20, D-01069 Dresden, Germany. E-mail: s.sanchez@ifw-dresden.de; Fax: +49 3514659782; Tel: +49 351 4659 845

^bNon-Equilibrium Chemical Physics, Physics Department, TU Munich, James-Frank-Str. 1, 85748 Garching, Germany

^cDepartment of Chemical and Biomolecular Engineering, Department of Chemistry, Johns Hopkins University, Baltimore, Maryland 21218, USA

^dMaterials Systems for Nanoelectronics, TU Chemnitz, 09107 Chemnitz, Germany

† Electronic supplementary information (ESI) available: Videos 1–4. See DOI: 10.1039/c2nr32798h

‡ These authors contributed equally to this work.

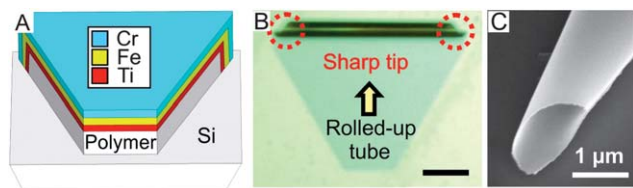


Fig. 1 Fabrication of ferromagnetic rolled-up microtubes with sharp tips. (A) Schematic representation of metallic nano-membranes consisting of Ti/Cr/Fe (5/5/5 nm) deposited in a trapezoid pattern for the fabrication of sharp tipped rolled-up microtubes. (B) Optical micrograph depicting the sharp tipped rolled-up ferromagnetic tubes in a trapezoid pattern (scale bar: 15 μm), and (C) scanning electron microscope image showing the sharp end of a typical microtool.

reported.^{28,29} An iron layer was employed to integrate the function of remote magnetic control into the microdevices, and Ti and Cr layers facilitated the roll-up process. After deposition, the samples were immersed in *N*-methyl-2-pyrrolidone for 30 minutes for the roll-up process. The rolled-up microtubes were then dried in a supercritical point dryer to avoid the surface-tension driven collapse of the thin metallic structures. The sharp tips of the microdrillers (Fig. 1B and C) are a consequence of the trapezoid pattern and the tilted rolled-up direction of the nanomembranes during etching of the sacrificial layer (Fig. 1B). The diameters of the microdrillers can be readily altered by varying the stress or material thickness of the sandwiched nanomembranes.^{28,29} In this study, we optimized the diameters for microdrillers ranging from 5 to 10 μm . Fig. 1C shows an SEM image of the sharp tip of a typical microdriller. Microdrillers were released from the substrate by gentle mechanical scratching and suspended into solutions containing a common soap (Fit GmbH) and water. The choice of soap in water was mainly utilized to minimize surface drag forces during the investigation of these dynamic microtools at different viscosities.

The incorporation of a thin ferromagnetic layer of Fe (5 nm) allows magnetic control over the motion of the microdrillers using a rotational external magnetic field (20 mT).¹⁴ Fig. 2A shows a sequence of optical microscopy images of a microdriller in solution located above a rotational magnetic field. The microdriller changes its rotational position from a horizontal to a vertical one (video 1 and 2 in the ESI†). This transition of the rotation mode is subject to a specific frequency threshold, which depends on the viscosity of the solution. Fig. 2A indicates the positions of the microdriller in, (a) static, (b) rotational horizontal, and (c) rotational vertical modes. For microtubes of 50 μm in length, consisting of Ti/Cr/Fe (5/5/5 nm, respectively) layers, it was observed that up to 300 rpm, the microtools started to rotate along the plane of the substrate (parallel to the surface, *i.e.*, x - y) and there was no change in their initial orientations in the z -plane.

Upon increase of the frequency of the magnetic field beyond a certain threshold, (blue plot in Fig. 2B), most of the microtools re-orient their long axis from parallel to the substrate to vertical. Further increase of the frequency did not change the rotational axis, and the microtools remained in the same acquired vertical mode (above the blue line: shadowed area in Fig. 2B). The necessary angular frequency required to cause the microdrillers to “stand up” was determined by measuring the threshold frequency in solutions of different viscosities, shown in Fig. 2B. The change in the dynamic

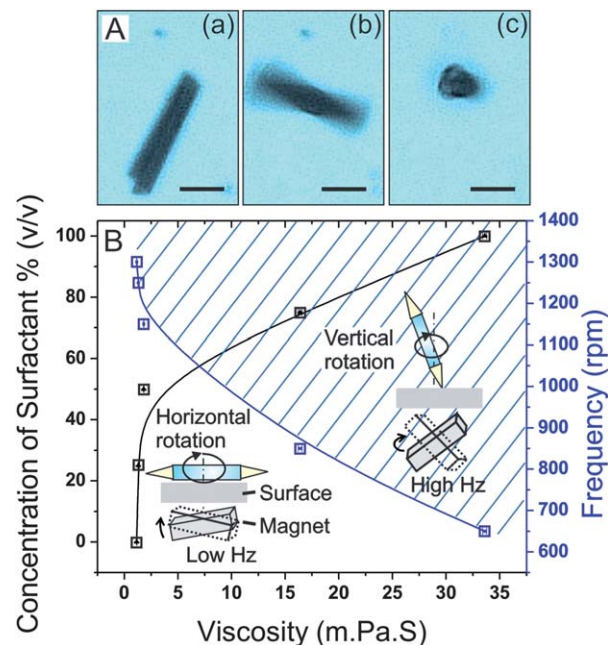


Fig. 2 Transition of the rotation of magnetic microdrillers from horizontal to vertical orientations. (A) Microscope images of the (a) static state, (b) planar and (c) vertical rotating microdrillers with respect to applied angular frequency (scale bar: 20 μm). (B) Concentration of the soap (% v/v) vs. viscosity (mPa s) at room temperature and threshold angular frequency (rpm) vs. viscosity (mPa s). The vertical rotation phase is shadowed and above the blue solid line while the planar phase is below. At these above plotted frequencies, the rolled up microtube changes its orientation from planar to vertical upright.

viscosity of the fluid at room temperature is directly correlated with the variation in the concentration of soap (Fig. 2B, black line). The threshold frequency for lifting the microtools and the viscosity of the solution are inversely proportional.

At a concentration of 50% (v/v) soap, a viscosity of 2.48 mPa s was achieved indicating that these tools could function in bodily fluids that have high viscosities (*e.g.* the viscosity of the blood (3.45 mPa s)).³⁰ A similar reorientation of rod-shaped magnetic gyroscopes in a dissipative environment from parallel to “standing-up” due to the different rotation frequency of the external magnetic field has been reported previously.³¹ Both the viscosity of the working solution and the applied angular frequency are important parameters for controlling the vertical/horizontal rotation of the microtools. The rotational magnetic field supplies power to the microtubes, which is dissipated by the rotation of the tubes in the viscous liquid and their interaction with the substrate. These two parameters together along with gravity are the three interactions determining the rotational orientation. At a higher angular frequency (*i.e.*, sufficient power supply), due to the tendency to minimize the potential energy of the system, the microtools rotate around the axis of smaller friction that is the long axis of tubular symmetry (standing position). The friction is proportional to the viscosity of the liquid. At a higher viscosity, friction destabilizes the planar phase in favor of the vertical phase, and as a result, a lower threshold frequency is needed to fuel the upright rotation of the microtubes.

When microtools are placed on hard planar surfaces (*e.g.* glass or silicon) and re-oriented to the upright rotation, they are able to



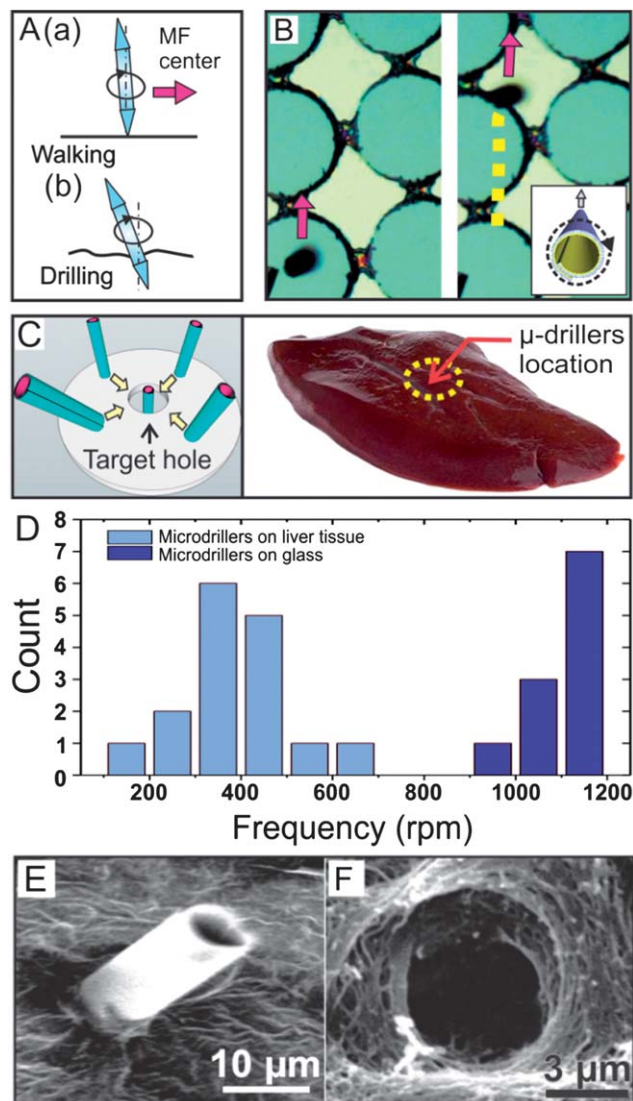


Fig. 3 (A) Walking and drilling microdrillers. (a) Fuel free motion of ferromagnetic tubes in vertical (stand-up) position walking towards the center of the magnetic field where the sample to be drilled is placed. (b) Schematic of a microdriller drilling at the site of interest. (B) Optical microscope images of tracked trajectory of a microdriller under the rotating magnetic field of 20 mT and a "walk" towards the center of the magnetic field. (C) Schematic graph showing the fuel-free motion of the microtools towards the center of the magnetic field and the drilling operation on porcine liver tissue. (D) The distribution of the stable rotation frequency of microtools on the tissue and on a rigid glass surface at the same applied external frequency of 1150 rpm. (E) SEM of a microdriller embedded into a pig liver section after drilling. (F) SEM image showing the drilled hole in the pig liver section after extracting the microdriller by a strong permanent magnet (500 mT).

"walk" towards the center of the rotational magnetic field. This type of motion is believed to be driven by both the external magnetic field as well as by the hydrodynamic interaction³⁰ between the tool and the surface. Fig. 3A shows a schematic of a microtool walking on the surface towards the center of the magnetic field and drilling a soft material (Fig. 3A(a) and (b)). Fig. 3B shows two optical microscopy images, indicating the tracked trajectory of motion of an individual microtool "walking" on a rigid Si wafer containing circular patterns. The dashed yellow line shows the tracked

trajectory of motion during 10 seconds. In the present work, this motion has been utilized to direct the microdrillers towards a specific location on substrates and on liver tissue *ex vivo*. To demonstrate the drilling operation (Fig. 3C), a pig liver section was placed at the centre of the magnetic field in a Petri dish containing microtools in the working solution (soapwater, 50% (v/v)). The angular frequency was increased to 1150 rpm, at which time the microtools switched their orientation from a horizontal to a vertical one. Thereafter, the microtools were guided to the desired locations and started the drilling operation, which lasted from tens of minutes to a few hours. In control experiments, we have proven that the microdrillers remain stable during such motions for several days (data not shown). It was observed that the microtools retain their upright orientation and the initial rotation frequency immediately after reaching the tissue, but they significantly slowed down in rotation frequency to a few hundred rpm after several minutes standing on the tissue (video 3†). However, that is not the case for microtools rotating on a rigid glass surface (video 4†), where they rotate at frequencies similar to the applied external rotation field (1150 rpm). Fig. 3D demonstrates that the rotation frequencies of microdrillers on the liver tissue are significantly slower than those on rigid surfaces where the drilling is impossible. Furthermore, the frequency distribution of the former is much wider than the latter, indicating a strong but non-uniform interaction between the sharp tip and the liver tissue accompanying the dissipation of a significant part of the energy. Such an interaction will increase the entropy production³⁰ of the microtube when rotating in a planar configuration and thus favours the vertical mode. Moreover, when located on the tissue, the microdrillers do not "walk" but remain stable at the placed position on the surface of tissue, possibly due to the compliant and rough surface. This kind of interaction is required to make the incision and facilitate the drilling operation during the course of several minutes (*ca.* 10 min), shown in Fig. 3E.

The SEM images of microtools embedded inside the liver tissue confirm the drilling operation (Fig. 3E). Some microdrillers reach a depth of *ca.* 25 μm as estimated by the length of the part of the 50 μm long microtube remaining outside the tissue. A permanent magnet was used to pull out the microtools so that the drilled holes in the liver section could be visualized. Fig. 3F shows an SEM image of a typical drilled micro-hole with an estimated diameter of *ca.* 6 μm, which is close to the diameter of the microtool.

Conclusions

We demonstrated the fabrication of 3D ferromagnetic microdrillers with sharp tips for drilling operations in soft biomaterials. The rolled-up microtools were formed from 2D nanomembranes of trapezia geometry. It is possible to dynamically switch the orientation of the microtool from a horizontal to a vertical position by changing the frequency of the external magnetic field and the viscosity of the solution. We presented magnetic control, drilling and guidance of fuel free microtools toward tissue samples *ex vivo*. We also demonstrated that such incisions can be performed in a fluid with viscosity similar to that of blood, which suggests applicability in the field of microrobotics for minimally invasive surgery. The surface friction between the sharp ends and the tissue is believed to facilitate the drilling operation. We expect that magnetic



microtools which can be precisely manipulated and controlled without the need for fuels will open up exciting possibilities and applications in miniaturized medicine and related fields in nanotechnology. In medical applications, an advantage of the tubular shape of the microtools is that the hollow cavity can be filled with drug loaded gels for more effective drug delivery into tumors and for clearing intravascular plaque.

Acknowledgements

This work was financially supported by the Volkswagen Foundation (86 362). D.H.G. acknowledges financial support from the Alexander von Humboldt Foundation. The authors thank J. Scheiter for viscosity measurements, D. Grimm for clean room support and D. Makarov for fruitful discussions.

Notes and references

- 1 S. Martel, O. Fefoloul, J.-B. Mathieu, A. Chanu, S. Tamaz, M. Mohammadi, M. Mankiewicz and N. Tabatabaei, *Int. J. Rob. Res.*, 2009, **28**, 1169.
- 2 T. G. Leong, C. L. Randall, B. R. Benson, N. Bassik, G. M. Stern and D. H. Gracias, *Proc. Natl. Acad. Sci. U. S. A.*, 2009, **106**, 703.
- 3 R. Fernandes and D. H. Gracias, *Mater. Today*, 2009, **12**, 14.
- 4 N. Bassik, A. Brafman, A. M. Zarafshar, M. Jamal, D. Luvsanjav, F. M. Selaru and D. H. Gracias, *J. Am. Chem. Soc.*, 2010, **132**, 16314.
- 5 A. A. Solovev, W. Xi, D. H. Gracias, S. M. Harazim, C. Deneke, S. Sanchez and O. G. Schmidt, *ACS Nano*, 2012, **6**, 1751.
- 6 S. Sengupta, M. E. Ibele and A. Sen, *Angew. Chem., Int. Ed.*, 2012, **51**, 8434.
- 7 T. E. Mallouk and A. Sen, *Sci. Am.*, 2009, **300**, 72.
- 8 S. Sanchez, A. A. Solovev, Y. Mei and O. G. Schmidt, *J. Am. Chem. Soc.*, 2010, **132**, 13144.
- 9 W. F. Paxton, K. C. Kistler, C. C. Olmeda, A. Sen, S. K. St. Angelo, Y. Cao, T. E. Mallouk, P. E. Lammert and V. H. Crespi, *J. Am. Chem. Soc.*, 2004, **126**, 13424.
- 10 M. Pumera, *Chem. Commun.*, 2011, **47**, 5637.
- 11 S. Sanchez, A. A. Solovev, S. Schulze and O. G. Schmidt, *Chem. Commun.*, 2011, **47**, 698.
- 12 S. Sanchez, A. A. Solovev, S. M. Harazim and O. G. Schmidt, *J. Am. Chem. Soc.*, 2011, **133**, 701.
- 13 D. Kagan, S. Campuzano, S. Balasubramanian, F. Kuralay, G.-U. Glehsig and J. Wang, *Nano Lett.*, 2011, **11**, 2083.
- 14 A. A. Solovev, S. Sanchez, M. Pumera, Y. F. Mei and O. G. Schmidt, *Adv. Funct. Mater.*, 2010, **20**, 2430.
- 15 J. Wang and W. Gao, *ACS Nano*, 2012, **6**, 5745.
- 16 W. Gao, A. Uygun and J. Wang, *J. Am. Chem. Soc.*, 2011, **134**, 897.
- 17 R. Laocharoensuk, J. Burdick and J. Wang, *ACS Nano*, 2008, **2**, 1069.
- 18 R. Liu and A. Sen, *J. Am. Chem. Soc.*, 2011, **133**, 20064.
- 19 W. Gao, A. Pei and J. Wang, *ACS Nano*, 2012, **6**, 8432.
- 20 S. Sanchez, A. N. Ananth, V. M. Fomin, M. Viehrig and O. G. Schmidt, *J. Am. Chem. Soc.*, 2011, **133**, 14860.
- 21 W. Gao, D. Kagan, O. S. Pak, C. Clawson, S. Campuzano, E. Chuluun-Erdene, E. Shipton, E. E. Fullerton, L. Zhang, E. Lauga and J. Wang, *Small*, 2012, **8**, 460.
- 22 W. Gao, K. M. Manesh, J. Hua, S. Sattayasamitsathit and J. Wang, *Small*, 2011, **7**, 2047.
- 23 A. Ghosh and P. Fischer, *Nano Lett.*, 2009, **9**, 2243.
- 24 S. Tottori, L. Zhang, F. Qiu, K. K. Krawczyk, A. Franco-Obregon and B. J. Nelson, *Adv. Mater.*, 2012, **24**, 811.
- 25 B. J. Nelson, I. K. Kaliakatsos and J. J. Abbott, *Annu. Rev. Biomed. Eng.*, 2010, **12**, 55.
- 26 L. Zhang, J. J. Abbott, L. Dong, B. E. Kratochvil, D. Bell and B. J. Nelson, *Appl. Phys. Lett.*, 2009, **94**, 064107.
- 27 O. G. Schmidt and K. Eberl, *Nature*, 2001, **168**, 410.
- 28 Y. F. Mei, G. Huang, A. A. Solovev, E. B. Ureña, I. Mönch, F. Ding, T. Reindl, R. K. Y. Fu, P. K. Chu and O. G. Schmidt, *Adv. Mater.*, 2008, **20**, 4085.
- 29 S. M. Harazim, W. Xi, C. K. Schmidt, S. Sanchez and O. G. Schmidt, *J. Mater. Chem.*, 2012, **22**, 2878.
- 30 Y. I. Cho and K. R. Kenney, *Biorheology*, 1991, **28**, 241–262.
- 31 P. Dhar, C. D. Swayne, T. M. Fischer, T. Kline and A. Sen, *Nano Lett.*, 2007, **7**, 1010.

